

Particle and Energy Flow Following Giant Edge Localised Modes in JET

R D Gill, B Alper, S ALi-Ashrad, A Cheetham¹, N Deliyannis,
A W Edwards, G M Fishpool, L C Ingesson, J Lingertat,
L Mayaux, L Porte², M Romanelli and R Simonini

JET Joint Undertaking, Abingdon, Oxfordshire, OX14 3EA, UK.

¹University of Canberra, P.O. Box 1, Belconnen, ACT 2616, Australia

²UCLA Department of Electrical Engineering, Los Angeles, USA .

Preprint of a paper to be submitted for publication in
Physics Review Letters

October 1997

"This document is intended for publication in the open literature. It is made available on the understanding that it may not be further circulated and extracts may not be published prior to publication of the original, without the consent of the Publications Officer, JET Joint Undertaking, Abingdon, Oxon, OX14 3EA, UK".

"Enquiries about Copyright and reproduction should be addressed to the Publications Officer, JET Joint Undertaking, Abingdon, Oxon, OX14 3EA".

Abstract

Giant elms play an important role in controlling the divertor tokamak edge plasma and cause the loss of a substantial fraction of the plasma energy and particles over a short time interval of $\approx 100\mu\text{s}$. This leads to a very high power loading of parts of the tokamak wall structure. The details of the loss processes are not understood. Using a set of highly time-resolved diagnostics, the flow of both energy and particles during giant edge localised modes (elms) has been determined for the first time. The soft X-ray measurements show a very rapid onset of the instability and have a remarkably complex structure. They prove that the plasma energy is deposited both in the divertor and other areas of the vessel, and that of the particles lost, many are recycled to well within the separatrix. The implications of the measurements for the elm instability mechanism and the design of tokamaks are discussed.

In tokamak configurations containing an X-point, the plasma is generally subject to an edge instability (elm) which adversely affects the overall plasma performance¹). Although the phenomenological properties of the elms are well known²), many of the details of their origin and structure are unclear. Giant (or type 1) elms have a particularly strong effect on the plasma as in these up to 10% of the plasma energy may be lost in $100\mu\text{s}$. In addition, they are often associated with a substantial and sudden drop in plasma confinement, and reduction in neutron production in deuterium discharges³). The large magnitude of these effects makes the giant elms particularly suitable for the determination of their detailed structure and time development, and the flow of energy and particles. New results on these processes have been obtained in JET

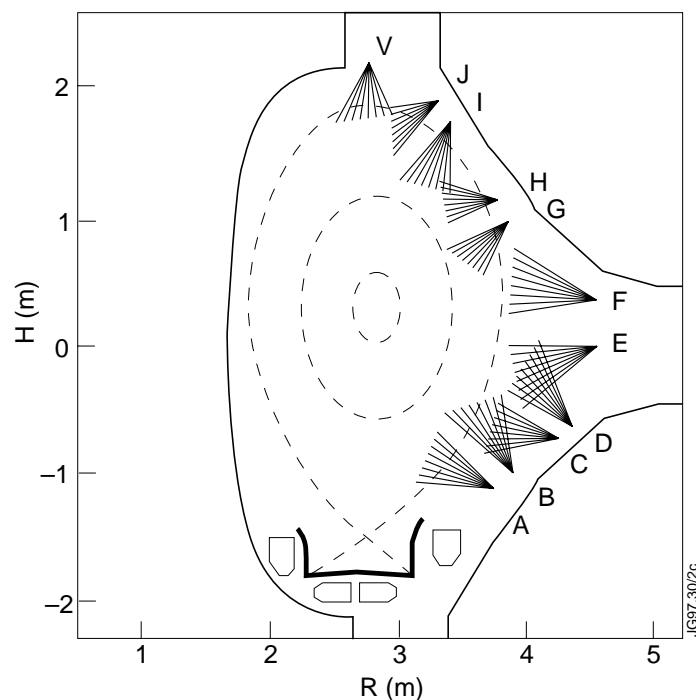


Fig. 1: Soft X-ray cameras in JET. Each camera has 18 detectors except V which has 35.

in the Mk I divertor with a very high time resolution ($10\mu\text{s}$) set of diagnostics in discharges with neutral beam heating. These include synchronized measurements of ECE, reflectometry, soft X-rays (Fig. 1), D_α , Langmuir probes and magnetics. Data taken with some of these in the divertor region for a giant elm (Fig. 2) shows the typical D_α and soft X-ray spike, and the rapid changes of ECE emission on the T_e trace. The diamagnetic loop determined a substantial loss of plasma energy ($\sim 7\%$ in this case).

The ECE measurement shows a very fast ($60\mu\text{s}$) T_e spike. This is often followed by a drop which continues for several ms. It is believed that the spike is caused either by the formation during the elm of a non-thermal electron distribution which modifies the absorption of the cyclotron radiation⁴⁾ or the scattering of pre-existing non-thermal electrons⁵⁾. Neither mechanism affects the plasma energy content or the X-ray emission. The dip is possibly due to the production at the plasma edge of a high density region following recycling of the particles lost in the elm.

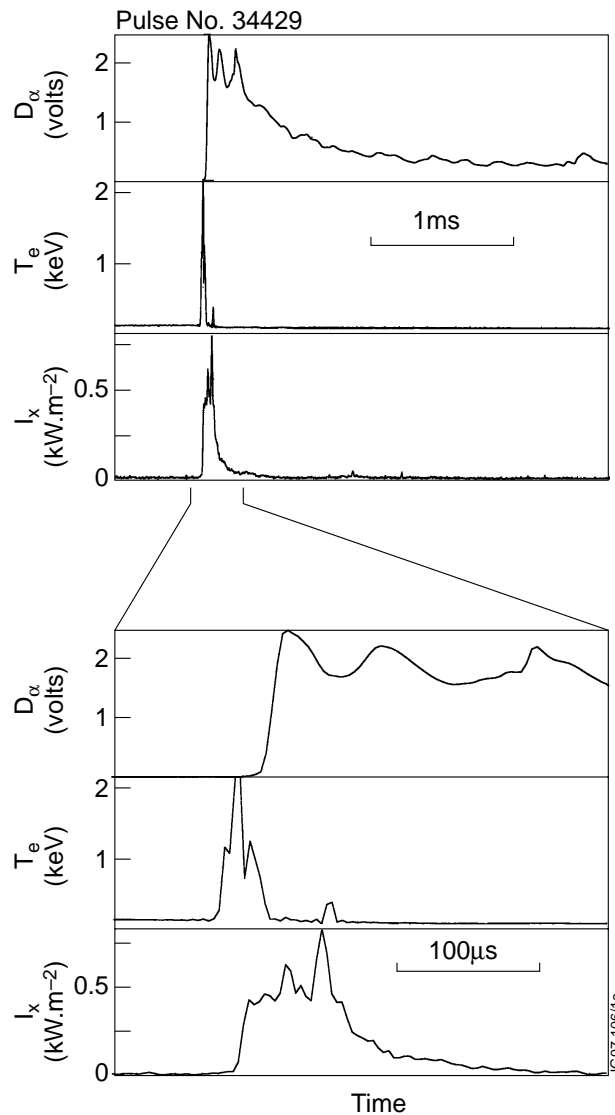


Fig. 2: D_α , T_e and X-ray intensity (all in arb units) in the divertor for a typical giant elm. Parameters are $B_f = 3.1T$, $I_p = 3MA$, T_e (plasma centre) = 11keV .

There do not generally seem to be any precursors to the elms although some of them occur during bursts of mhd activity measured by the magnetics at $f = 25 - 30\text{kHz}$. The magnetics also show that the plasma position moves only 1-2cm during the elm. Complicated changes are seen on the loop voltage and plasma current signals and I_p drops rapidly by $\approx 1\%$. The reflectometer observes a continuous coherent mode at about 25kHz, possibly outside the separatrix, which changes at the elm to broadband activity. An infrared camera which views the divertor target plates shows, with time resolution of $200\mu\text{s}$, that the separation of the strike points increases during an elm from 20 to 36cm although the time at which this occurs is undetermined.

Very detailed measurements on the elms come from the 12 soft X-ray cameras⁶⁾ of which 11 are in one poloidal plane. Each of these views the plasma through a $250\mu\text{m}$ Be foil (energy threshold 2.2 keV) with 18 channels (except the vertical camera which has 35) and spatial resolution of about 12 cm at the wall. Pronounced and rapid flashes of X-rays (Fig. 3) are seen during the elm with the intensity doubling in some central channels of the vertical camera. The view of the vertical camera into the divertor region shows four characteristic bands and the views of this same region from other cameras prove that the solid material boundary is the source of the emission (Fig. 4).

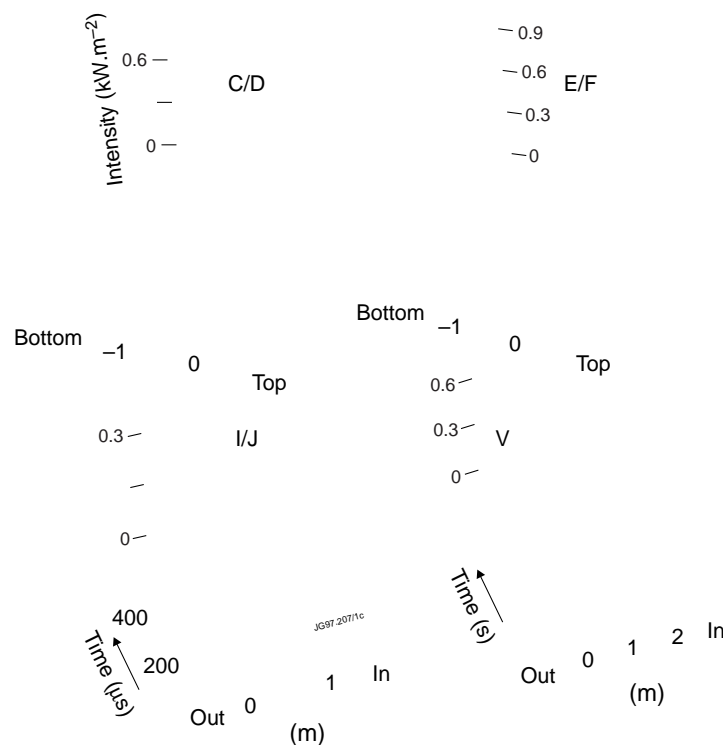


Fig. 3: X-ray emission from several cameras during the giant elm. The intensities just before the elm have been subtracted for each channel.

The two central bands correspond to the divertor strike points although they are shifted away from the equilibrium strike points by

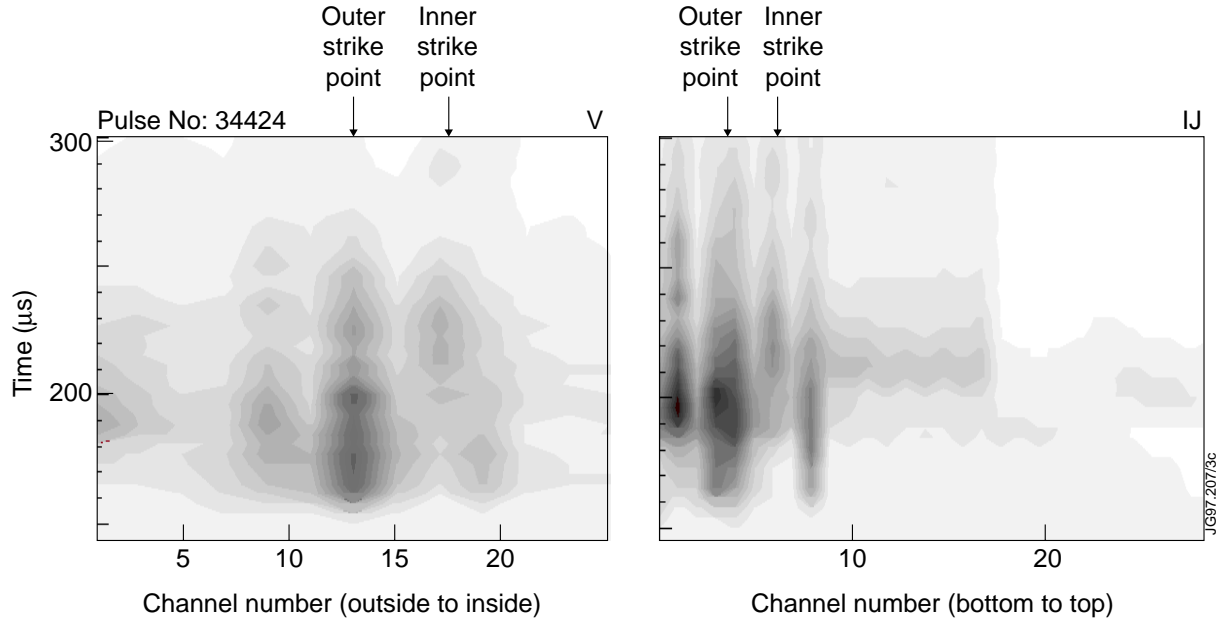


Fig. 4: Contour plot of X-ray intensity observed by camera V and I, J. The data shows the changes during the elm as the emission profiles just before the elm have been subtracted. The four characteristic areas of emission are seen.

10-14 cm. The two outer bands correspond to the outer shoulders of the divertor structure. Parts of the divertor are in shadows because of the magnetic field structure and this accounts for the outer two regions of reduced emission (Fig. 5). The central region of reduced emission corresponds to the private flux region. Tomographic analysis of the data has also confirmed the localisation of the radiation. Observations in a camera equivalent to V at another toroidal location show that the pattern is generally similar but toroidally asymmetric.

The observation of the X-rays requires the existence of the electrons with keV energies. These must originate well within the separatrix and be lost during the elm instability. This is quite possible as the electron temperature rises rapidly to 3 keV within 10cm of the separatrix. The X-rays are then produced by bremsstrahlung from the divertor plates and walls when the electrons flow out through the scrape off layer. This can produce the observed X-ray intensity even though this process is rather inefficient. For an electron with initial energy E impinging onto a surface with atomic

number Z the fraction radiated is:

$$R_B = \frac{\text{Total radiated as bremsstrahlung}}{\text{Initial electron energy}} = 3 \times 10^{-4} \frac{EZ}{m_e c^2}$$

where $m_e c^2$ is the rest energy of the electron. If $E = 2$ keV and $Z = 6$ then $R_B = 7 \times 10^{-6}$. However, during the elm, the power generated by the loss of plasma is extremely high so that the

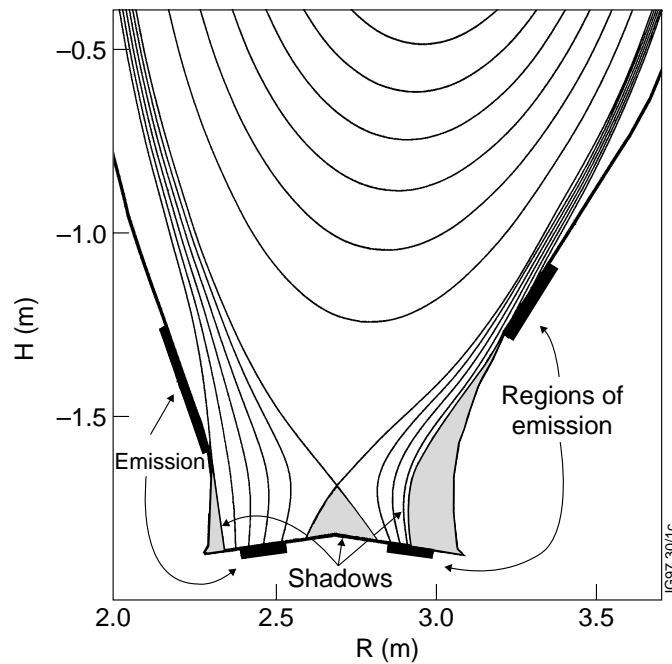


Fig. 5: Regions of X-ray emission near the divertor and shadowed regions produced by the interaction of the magnetic field structure with the torus boundary are shown.

power appearing in X-rays can easily be comparable with that coming from the quiescent plasma. For example, if 700kJ is lost in 10^{-4} s and deposited over a toroidal band of width 0.1m in the divertor an X-ray intensity of 26kW/m^2 would be observed. Calculations show⁷⁾ that the effect of the Be filters would reduce this by about an order of magnitude to make it comparable to the observed values. It follows that the soft X-ray signals in the divertor give a footprint of the energy loss of the hot plasma during the elm and show that energy is deposited over a considerable area of the vessel outside the divertor.

Strong X-ray flashes are also seen from localised regions up to 15cm within the separatrix and the regions of emission have been determined from tomographic reconstructions of the data (Fig 6a). These regions are close to the two points of the limiter which are closest to the separatrix, so that some of the plasma expelled into the scrape-off layer will interact with the limiters and the deuterium ions will be reflected and recycled as neutrals back into the plasma. The enhanced local density will increase the X-ray emission. The points of interaction of the limiter are not viewed by the X-ray cameras. As the divertor measurements imply the existence of keV electrons in the scrape-off layer, it is reasonable to assume that the escaping deuterons will also have a similar energy. On hitting the limiter these will be reflected with reduced intensity and energy, but still with quite high energy compared with the eV energies values normally possessed by recycling neutrals. This will give them considerably greater penetration length into the plasma and approximate estimates show that substantial numbers of these neutrals could penetrate the necessary 0.15m seen in the measurements. This idea has been checked with the NIMBUS code⁸⁾ where a source of neutrals at energy 0.3 keV has been placed at the limiter tips. The

ionization source within the plasma shows a poloidal spatial variation very similar to the observation (Fig. 6b) but radially the X-ray emission drops to zero at the plasma edge because of the low temperature.

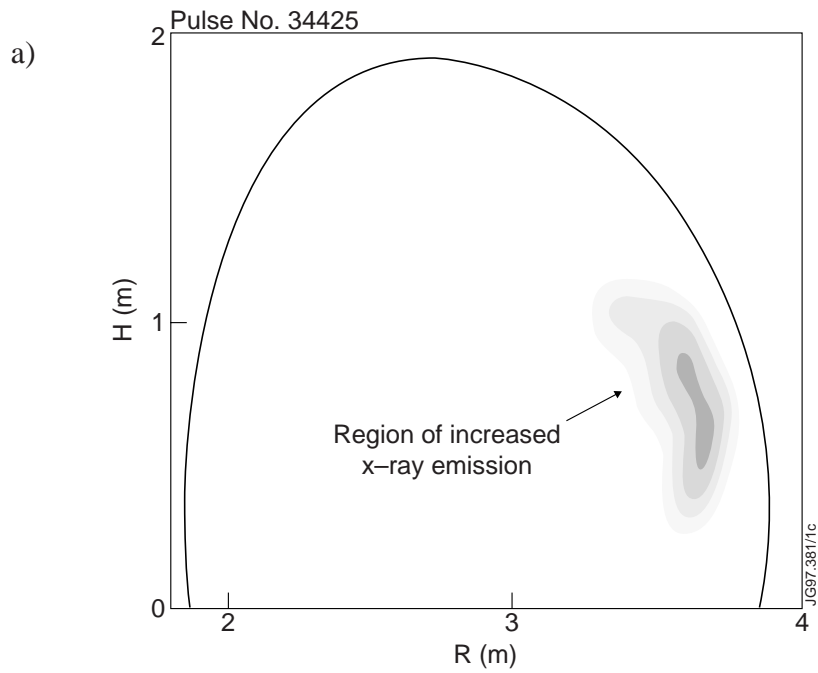


Fig. 6(a): Tomographic reconstruction of background subtracted X-ray signals near the upper tip of the outer limiter. The region of intense emission from within the plasma stands out clearly.

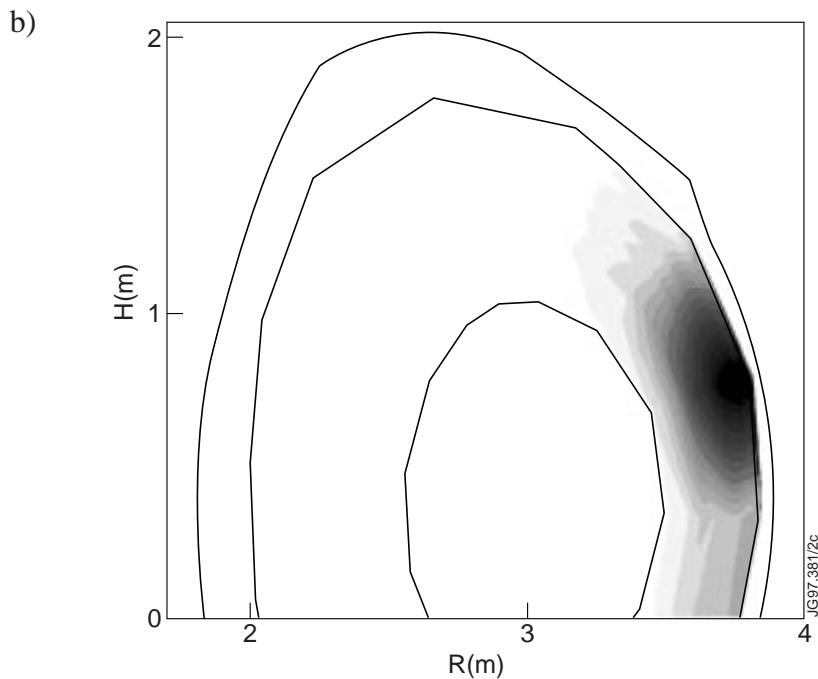


Fig. 6(b): Calculated ionization source for the same region.

The magnitude of the increased X-ray emission is also well accounted for in an approximate estimate as the proposed mechanism is an efficient way of concentrating the plasma expelled

into the scrape-off layer within the plasma and increasing the density locally. The estimate assumes that the fraction of the total plasma particles lost into the scrape-off layer is the same as the fraction of the energy which is lost and shows that the X-ray intensity could be locally doubled.

It has already been mentioned that there is generally a lack of precursor activity to the elm and many of the diagnostics show a rapid onset in $\geq 10\mu\text{sec}$. In particular the soft X-ray signals have a rapid rise time ($5\mu\text{s}$) and the growth time of the instability must be at least this fast. The flow of plasma into the divertor must be determined by the mean ion sound velocity (\bar{v}_i) and the very rapid growth rate (t_r) implies that the plasma displaced onto open field lines has not travelled a distance further than $\ell = \bar{v}_i t_r$. This corresponds to a rather short distance projected into the poloidal plane of $\bar{v}_i t_r B_\theta / B_\phi \approx 0.5\text{m}$ and implies that the first observed plasma in the divertor has originated from the bottom of the plasma near the X-point. Similarly, some of the limiter recycled plasma must have been expelled into the SOL close to this limiter. The rapid rise in X-ray emission in both the divertor region and the recycling feature implies that the instability expels plasma close to both these regions.

The results are completely consistent with the idea that plasma from a layer about 6cm thick is exchanged by the elm instability into a layer outside the separatrix and then flows down into the divertor region or onto a limiter. The large wall area of the interaction is due to the six-fold flux expansion near the X-point, compared with the outer mid-plane. The loss of this layer is also confirmed by the changes in the X-ray emission profiles at the edge. Although the behaviour of the edge cannot be followed during the elm because of the X-ray flashes, after the elm it is seen that the edge has moved inwards and a layer of about 6 cm has been lost from the outer region. Together with the interpretation of the X-ray flashes this shows that the instability leads to an interchange of a layer of plasma with a temperature of $\sim 2\text{keV}$ and about 6cm thick into a layer outside the separatrix where it is then lost down into the divertor region.

The decay times of the D_α and X-ray signals are different. The D_α signal decays over $180\mu\text{s}$ or more and this corresponds to the time taken to drain the scrape-off layer of ions. The X-ray signal decays faster, in $\sim 60\mu\text{s}$. This time is comparable with the electron energy exchange time and it is believed that cold electrons are produced in the scrape off layer following the ionization due to the production of impurity ions produced at the divertor plate. This idea is plausible as it is seen that the giant elm is accompanied by a considerable rise in the plasma Z_{eff} and density.

Even though very detailed observations have been made it is difficult to correlate them with existing theoretical models which need to be extended to follow through the non-linear consequences of the initial instability. Most models will have difficulty in accounting for the very rapid onset of the elm.

It is generally accepted that the giant elms occur when the pressure gradient reaches the critical value for the onset of ideal ballooning modes²⁾ and the observed very rapid observed instability growth time would suggest ideal rather than resistive modes. These modes would be expected to expel most power onto the outer divertor plate in disagreement with the observation. However, this difficulty could be overcome if the ballooning mode was coupled to a low n-number instability, which might also give rise to the observed toroidal asymmetry.

An alternative might be the external ideal kink mode suggested by Manickam⁹⁾ in which the plasma edge current together with the edge pressure gradient play important roles. This instability is often dominated by a single helicity with $m/n > q$ (edge) which could produce the observed toroidal variation.

The present results do not seem to be in agreement with the model of Kerner et al¹⁰⁾ in which the elm is seen as the consequence of an ideal instability at the plasma X-point followed by the flow of plasma from within the separatrix onto the divertor plates. The principal discrepancy is the observation that no plasma flows into the private flux region which is always in a shadow. The observation of fast interactions with the upper limiter are also in disagreement.

In relation to the design and operation of tokamaks the results have consequences for operation modes which include giant elms.

- (a) The plasma expelled in the elm is spread over a considerable area of the tokamak walls outside the divertor region and these areas need protection from the high heat fluxes. However, this spreading has the desirable effect of reducing the heat load per unit area.
- (b) The tokamak should be operated with the separatrix well away from the plasma boundary so that there is an adequate volume outside the separatrix for plasma expelled by the elm to flow down into the divertor region and not onto the vessel wall in an uncontrolled way.

ACKNOWLEDGEMENTS:

We would like to thank J Wesson and P Thomas for useful comments on this work.

REFERENCES

- 1) F Wagner *et al.* Phys. Rev. Lett., **49** 1408 (1982).
- 2) H Zohm. Plasma Physics Controlled Fusion, **38**, 105 (1996)
H Zohm, Plasma. Physics Controlled Fusion, **38**, 1213 (1996)
- 3) J Wesson and B Balet, Physics Review Letters **77**, 5214 (1996).
- 4) A Janos, J Hastie, K McGuire and E Fredrickson, Plasma Physics and Controlled Fusion **38**, 1373 (1996).
- 5) L Porte, Ph.D. Thesis, University of Strathclyde (1993)
- 6) B Alper *et al.*, Review of Scientific Instruments **68**, 778 (1997)
- 7) R D Gill, JET-IR(97)01
- 8) R Simonini, G Corrigan, G Radford, J Spence, A Taroni, Plasma Physics Controlled Fusion, **34**, 368 (1994)
- 9) J. Manickam, Phys. Fluids, **B4**, 1901 (1992)
- 10) W. Kerner, O. Pogutse, R. van der Linden and B. Schunke, Plasma Physics and Controlled Fusion, Plasma Physics Controlled Fusion, **39**, 757 (1997).